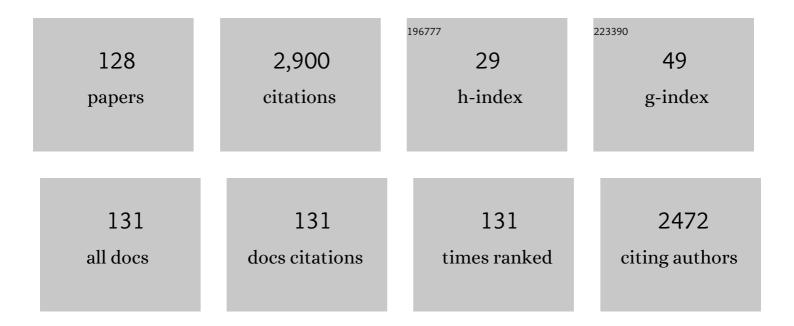
## Tohru Kawamoto

List of Publications by Year in descending order

Source: https://exaly.com/author-pdf/4303311/publications.pdf Version: 2024-02-01



#	Article	IF	CITATIONS
1	Apparatus for ammonia removal in livestock farms based on copper hexacyanoferrate granules. Biosystems Engineering, 2022, 216, 98-107.	1.9	8
2	The development of a rapid monitoring method for radiocesium in seawater in the Fukushima region. Environmental Science: Water Research and Technology, 2022, 8, 1547-1560.	1.2	3
3	Thermal Decomposition Behavior of Prussian Blue in Various Conditions. Materials, 2021, 14, 1151.	1.3	11
4	Selective Adsorption of Potassium in Seawater by CoHCF Thin Film Electrode and Its Electrochemical Desorption/Regeneration. Materials, 2021, 14, 3592.	1.3	1
5	Life Cycle Assessment of Nitrogen Circular Economy-Based NOx Treatment Technology. Sustainability, 2021, 13, 7826.	1.6	8
6	Ammonium removal and recovery from sewage water using column-system packed highly selective ammonium adsorbent. Environmental Pollution, 2021, 284, 117495.	3.7	8
7	Ammonium salt production in NH3-CO2-H2O system using a highly selective adsorbent, copper hexacyanoferrate. Environmental Pollution, 2021, 288, 117763.	3.7	8
8	Harvesting a Solid Fertilizer Directly from Fetid Air. ACS Sustainable Chemistry and Engineering, 2021, 9, 16865-16869.	3.2	6
9	Cesium uptake ability of a nonwoven fabric supporting iron hexacyanoferrate nanoparticles from solutions of coexisting alkali metal ions. Inorganica Chimica Acta, 2020, 503, 119401.	1.2	2
10	Synthesis and characterization of mixed Co-Zn-ZIF for arsenic(V) adsorption. Inorganica Chimica Acta, 2020, 502, 119311.	1.2	15
11	H2O2-sensing abilities of mixed-metal (Fe-Ni) Prussian blue analogs in a wide pH range. Inorganica Chimica Acta, 2020, 502, 119314.	1.2	9
12	Unique adsorption and desorption behaviour of ammonia gas at heating temperature using the Prussian blue analogue Zn3[Co(CN)6]2. Inorganica Chimica Acta, 2020, 501, 119273.	1.2	5
13	Single Open Sites on Fe <sup>II</sup> Ions Stabilized by Coupled Metal Ions in CN-Deficient Prussian Blue Analogues for High Catalytic Activity in the Hydrolysis of Organophosphates. Inorganic Chemistry, 2020, 59, 16000-16009.	1.9	6
14	Electrochromic properties of sputter-deposited rhodium oxide thin films of varying thickness. Thin Solid Films, 2020, 709, 138226.	0.8	9
15	FeNi-Layered Double-Hydroxide Nanoflakes with Potential for Intrinsically High Water-Oxidation Catalytic Activity. ACS Applied Energy Materials, 2020, 3, 9040-9050.	2.5	16
16	Trace Ammonia Removal from Air by Selective Adsorbents Reusable with Water. ACS Applied Materials & Interfaces, 2020, 12, 15115-15119.	4.0	27
17	Green fabrication of a complementary electrochromic device using water-based ink containing nanoparticles of WO <sub>3</sub> and Prussian blue. RSC Advances, 2020, 10, 2562-2565.	1.7	20
18	Roll-to-roll production of Prussian blue/Pt nanocomposite films for flexible gasochromic applications. Inorganica Chimica Acta, 2020, 505, 119466.	1.2	5

#	Article	IF	Citations
19	Electrochromic properties of WO <sub>3</sub> thin films fabricated by magnetron sputtering, ion plating, and spin coating: A comparative investigation. Journal of the Ceramic Society of Japan, 2020, 128, 381-386.	0.5	7
20	Decontamination of very dilute Cs in seawater by a coagulation–precipitation method using a nanoparticle slurry of copper hexacyanoferrate. Environmental Science: Water Research and Technology, 2019, 5, 1328-1338.	1.2	12
21	Pre-enrichment of radioactive cesium in muddy water separated into suspended and dissolved substances for trace analysis. Water Research, 2019, 154, 28-33.	5.3	3
22	Interpretation of the Role of Composition on the Inclusion Efficiency of Monovalent Cations into Cobalt Hexacyanoferrate. Chemistry - A European Journal, 2019, 25, 5950-5958.	1.7	6
23	One million cyclable blue/colourless electrochromic device using K <sub>2</sub> Zn <sub>3</sub> [Fe(CN) <sub>6</sub> ] <sub>2</sub> nanoparticles synthesized with a micromixer. RSC Advances, 2019, 9, 41083-41087.	1.7	5
24	Differences in NH3 gas adsorption behaviors of metal-hexacyanoferrate nanoparticles (M [FeII(CN)6]) Tj ETQq0	0 0 <sub>1</sub> .gBT /0	Overlock 10 Tf
25	Prussian Blue Nanoparticles and Nanocomposites for Cs Decontamination. , 2019, , 217-242.		4
26	High contrast gasochromism of wet processable thin film with chromic and catalytic nanoparticles. Journal of Materials Chemistry C, 2018, 6, 4760-4764.	2.7	9
27	Highly Sensitive and Exceptionally Wide Dynamic Range Detection of Ammonia Gas by Indium Hexacyanoferrate Nanoparticles Using FTIR Spectroscopy. Analytical Chemistry, 2018, 90, 4856-4862.	3.2	11
28	High-capacity and selective ammonium removal from water using sodium cobalt hexacyanoferrate. RSC Advances, 2018, 8, 34573-34581.	1.7	18
29	Adsorption ofÂng L <sup>â^'1</sup> -level arsenic by ZIF-8 nanoparticles: application to the monitoring of environmental water. RSC Advances, 2018, 8, 36360-36368.	1.7	7
30	Effects of the variation of metal substitution and electrolyte on the electrochemical reaction of metal hexacyanoferrates. RSC Advances, 2018, 8, 37356-37364.	1.7	15
31	Unveiling Cs-adsorption mechanism of Prussian blue analogs: Cs <sup>+</sup> -percolation <i>via</i> vacancies to complete dehydrated state. RSC Advances, 2018, 8, 34808-34816.	1.7	55
32	An Apparatus for Vertical Distribution Measurement of Radiocaesium in Pond Sediment Using Commercially Available Parts. Radioisotopes, 2018, 67, 329-338.	0.1	0
33	Multilayered Electrochromic Films of Metal Hexacyanoferrates Nanoparticles. International Journal of Electrochemical Science, 2018, 13, 4243,4250	0.5	1

34	High performance sorption and desorption behaviours at high working temperatures of ammonia gas in a cobalt-substituted Prussian blue analogue. Chemical Communications, 2018, 54, 11961-11964.	2.2	22
35	Trace Alcohol Adsorption by Metal Hexacyanocobaltate Nanoparticles and the Adsorption Mechanism. Journal of Physical Chemistry C, 2018, 122, 11918-11925.	1.5	10

Fineâ€Tunable Electronic Energy Levels of Mixedâ€Metal Prussianâ€Blue Alloy Nanoparticles. ChemNanoMat, 2017, 3, 288-291. 1.5 36 7

#	Article	IF	CITATIONS
37	Analysis of Cs-adsorption behavior using a column filled with microcapsule beads of potassium copper hexacyanoferrate. Journal of Nuclear Science and Technology, 2017, 54, 1157-1162.	0.7	3
38	Cobalt hexacyanoferrate nanoparticles for wet-processed brown–bleached electrochromic devices with hybridization of high-spin/low-spin phases. Journal of Materials Chemistry C, 2017, 5, 8921-8926.	2.7	20
39	Inversion analysis on vertical radiocesium distribution in pond sediment from γ-ray count measurement. Journal of Environmental Radioactivity, 2017, 175-176, 158-163.	0.9	7
40	Cesium removal from drinking water using Prussian blue adsorption followed by anion exchange process. Separation and Purification Technology, 2017, 172, 147-151.	3.9	24
41	Battery-type column for caesium ions separation using electroactive film of copper hexacyanoferrate nanoparticles. Separation and Purification Technology, 2017, 173, 44-48.	3.9	11
42	Radioactive cesium decontamination technology for ash. Synthesiology, 2016, 9, 139-154.	0.2	2
43	Prospective Application of Copper Hexacyanoferrate for Capturing Dissolved Ammonia. Industrial & Engineering Chemistry Research, 2016, 55, 6708-6715.	1.8	25
44	Historical Pigment Exhibiting Ammonia Gas Capture beyond Standard Adsorbents with Adsorption Sites of Two Kinds. Journal of the American Chemical Society, 2016, 138, 6376-6379.	6.6	126
45	Water processable Prussian blue–polyaniline:polystyrene sulfonate nanocomposite (PB–PANI:PSS) for multi-color electrochromic applications. Journal of Materials Chemistry C, 2016, 4, 10293-10300.	2.7	43
46	Decomposition of Iron Hexacyanoferrate Microcapsule Beads Using Superheated Steam. Chemistry Letters, 2016, 45, 670-672.	0.7	2
47	Radiocesium removal system for environmental water and drainage. Water Research, 2016, 107, 29-36.	5.3	5
48	Comparative study of the factors associated with the application of metal hexacyanoferrates for environmental Cs decontamination. Chemical Engineering Journal, 2016, 283, 1322-1328.	6.6	76
49	Application of Prussian blue nanoparticles for the radioactive Cs decontamination in Fukushima region. Journal of Environmental Radioactivity, 2016, 151, 233-237.	0.9	49
50	Assessment of the measures for the extraction or fixation of radiocesium in soil. Geoderma, 2016, 267, 169-173.	2.3	12
51	Improved adsorption properties of granulated copper hexacyanoferrate with multi-scale porous networks. RSC Advances, 2016, 6, 16234-16238.	1.7	31
52	Development of a copper-substituted, Prussian blue-impregnated, nonwoven cartridge filter to rapidly measure radiocesium concentration in seawater. Journal of Nuclear Science and Technology, 2016, 53, 1243-1250.	0.7	16
53	Radioactive cesium removal from ash-washing solution with high pH and high K+-concentration using potassium zinc hexacyanoferrate. Chemical Engineering Research and Design, 2016, 109, 513-518.	2.7	26
54	Technology for radioactive cesium decontamination from ash. Synthesiology, 2016, 9, 139-153.	0.2	4

#	Article	IF	CITATIONS
55	Rapid quantification of radiocesium dissolved in water by using nonwoven fabric cartridge filters impregnated with potassium zinc ferrocyanide. Journal of Nuclear Science and Technology, 2015, 52, 792-800.	0.7	42
56	Simultaneous Enhancement of Cs-Adsorption and Magnetic Properties of Prussian Blue by Thermal Partial Oxidation. Bulletin of the Chemical Society of Japan, 2015, 88, 69-73.	2.0	10
57	Sequential Structural Control of Open-Framework Nanoparticles Both in Dispersion and in Film for Electrochemical Performance Tuning. Bulletin of the Chemical Society of Japan, 2015, 88, 1561-1566.	2.0	3
58	Prussian blue (PB) granules for cesium (Cs) removal from drinking water. Separation and Purification Technology, 2015, 143, 146-151.	3.9	74
59	Efficient synthesis of size-controlled open-framework nanoparticles fabricated with a micro-mixer: route to the improvement of Cs adsorption performance. Green Chemistry, 2015, 17, 4228-4233.	4.6	37
60	Numerical evaluation of Cs adsorption in PB column by extended Langmuir formula and one-dimensional adsorption model. Journal of Radioanalytical and Nuclear Chemistry, 2015, 303, 1287-1290.	0.7	4
61	Column study on electrochemical separation of cesium ions from wastewater using copper hexacyanoferrate film. Journal of Radioanalytical and Nuclear Chemistry, 2015, 303, 1491-1495.	0.7	21
62	Accelerated coloration of electrochromic device with the counter electrode of nanoparticulate Prussian blue-type complexes. Electrochimica Acta, 2015, 163, 288-295.	2.6	41
63	Effective removal of hexacyanoferrate anions using quaternary amine type ion exchange resin. Journal of Environmental Chemical Engineering, 2015, 3, 2448-2452.	3.3	5
64	Prussian blue non-woven filter for cesium removal from drinking water. Separation and Purification Technology, 2015, 153, 37-42.	3.9	45
65	Variation in available cesium concentration with parameters during temperature induced extraction of cesium from soil. Journal of Environmental Radioactivity, 2015, 140, 78-83.	0.9	30
66	Monitoring low-radioactivity caesium in Fukushima waters. Environmental Sciences: Processes and Impacts, 2014, 16, 28-32.	1.7	17
67	Adsorption removal of cesium from drinking waters: A mini review on use of biosorbents and other adsorbents. Bioresource Technology, 2014, 160, 142-149.	4.8	181
68	Proton-exchange mechanism of specific Cs+ adsorption via lattice defect sites of Prussian blue filled with coordination and crystallization water molecules. Dalton Transactions, 2013, 42, 16049.	1.6	198
69	Selective removal of cesium ions from wastewater using copper hexacyanoferrate nanofilms in an electrochemical system. Electrochimica Acta, 2013, 87, 119-125.	2.6	114
70	Thermodynamics and Mechanism Studies on Electrochemical Removal of Cesium Ions from Aqueous Solution Using a Nanoparticle Film of Copper Hexacyanoferrate. ACS Applied Materials & Interfaces, 2013, 5, 12984-12990.	4.0	61
71	Growth of Pt Subnano Clusters on Limited Surface Areas of Prussian Blue Nanoparticles. Journal of Inorganic and Organometallic Polymers and Materials, 2013, 23, 216-222.	1.9	4
72	Rapid measurement of radiocesium in water using a Prussian blue impregnated nonwoven fabric. Journal of Nuclear Science and Technology, 2013, 50, 674-681.	0.7	49

#	Article	IF	CITATIONS
73	Dealing with the Aftermath of Fukushima Daiichi Nuclear Accident: Decontamination of Radioactive Cesium Enriched Ash. Environmental Science & Technology, 2013, 47, 3800-3806.	4.6	88
74	Improvement of redox reactions by miniaturizing nanoparticles of zinc Prussian blue analog. Applied Physics Letters, 2013, 102, .	1.5	12
75	Efficient Cesium Adsorbent Using Prussian Blue Nanoparticles Immobilized on Cotton Matrices. Chemistry Letters, 2012, 41, 1473-1474.	0.7	47
76	Removal of Cesium from Aqueous Solutions by Copper Hexacyanoferrate Membrane Coated Electrodes in a Electrochemical Adsorption System. Procedia Engineering, 2012, 44, 1728-1730.	1.2	1
77	Preparation of electrochromic Prussian blue nanoparticles dispersible into various solvents for realisation of printed electronics. Green Chemistry, 2012, 14, 1537.	4.6	59
78	Preparation of a film of copper hexacyanoferrate nanoparticles for electrochemical removal of cesium from radioactive wastewater. Electrochemistry Communications, 2012, 25, 23-25.	2.3	54
79	Synthesis of Water-Dispersible Copper Hexacyanoferrate Nanoparticles and Electrochromism of the Thin Films. Molecular Crystals and Liquid Crystals, 2011, 539, 18/[358]-22/[362].	0.4	11
80	Systematic Bathochromic Shift of Charge-transfer Bands of Mixed-metal Prussian-blue Nanoparticles Depending on Their Composition Ratios of Fe and Ni. Chemistry Letters, 2010, 39, 762-763.	0.7	18
81	Dispersion Control of Surface-charged Prussian Blue Nanoparticles into Greener Solvents. Chemistry Letters, 2010, 39, 138-139.	0.7	11
82	Electrochemical control of the elution property of Prussian blue nanoparticle thin films: mechanism and applications. Physical Chemistry Chemical Physics, 2009, 11, 10500.	1.3	11
83	Metal hexacyanochromate coordination nanopolymers: Surface ligand effect on their magnetism. Chemical Physics Letters, 2009, 480, 231-236.	1.2	2
84	Preparation of Yellow Core–Blue Shell Coordination Polymer Nanoparticles Using Active Surface Coordination Sites on a Prussian-blue Analog. Chemistry Letters, 2009, 38, 1058-1059.	0.7	16
85	Electrochromic Thin Film Fabricated Using a Water-Dispersible Ink of Prussian Blue Nanoparticles. Japanese Journal of Applied Physics, 2008, 47, 1242.	0.8	42
86	Electrochromic Thin Film of Water-Dispersible Prussian-Blue Nanoparticles. IEICE Transactions on Electronics, 2008, E91-C, 1887-1888.	0.3	7
87	Electrochromic Thin Film of Prussian Blue Nanoparticles Fabricated using Wet Process. Japanese Journal of Applied Physics, 2007, 46, L945.	0.8	51
88	Simple synthesis of three primary colour nanoparticle inks of Prussian blue and its analogues. Nanotechnology, 2007, 18, 345609.	1.3	163
89	Monte Carlo simulations of an Ising-like model for photoinduced spin-state switching in nanoparticles of transition metal complexes. Journal of Physics: Conference Series, 2005, 21, 56-60.	0.3	3
90	Uniaxial strain study in purely organic ferromagnet α-TDAE-C60 – Mechanism and structure. Polyhedron, 2005, 24, 2173-2175.	1.0	7

#	Article	IF	CITATIONS
91	Fixed spin effect on a phase switching of an Ising model under constant excitation: Study for impurity effect on photoinduced spin-state switching in transition metal complexes. Polyhedron, 2005, 24, 2676-2679.	1.0	2
92	Adsorption States of Dialkyl Ditelluride Autooxidized Monolayers on Au(111). Langmuir, 2005, 21, 3344-3353.	1.6	22
93	Thermal hysteresis loop of the spin-state in nanoparticles of transition metal complexes: Monte Carlo simulations on an Ising-like model. Chemical Communications, 2005, , 3933.	2.2	59
94	A Model of a Switching Molecular Junction with a Ring-shaped Molecule. Journal of the Physical Society of Japan, 2005, 74, 686-689.	0.7	0
95	Simulations with an Ising-like Model for Dynamical Phase Transitions under Strong Excitation. Journal of the Physical Society of Japan, 2004, 73, 3471-3478.	0.7	10
96	Magnetism of α- and β-TDAE-C60. Journal of Magnetism and Magnetic Materials, 2004, 272-276, E215-E216.	1.0	5
97	Dynamical phase transition under photo-excitation in a spin-crossover complex. Journal of Luminescence, 2004, 108, 229-232.	1.5	4
98	STM images of molecules on a metallic surface: a fast calculation based on a self-consistent semiempirical molecular orbital method. Physical Chemistry Chemical Physics, 2004, 6, 4913.	1.3	2
99	Stability of the staging structure of charge-transfer complexes showing a neutral–ionic transition. Physical Review B, 2004, 70, .	1.1	10
100	Electronic states in magnetic fullerides studied by ESR under pressure. Synthetic Metals, 2003, 133-134, 695-696.	2.1	2
101	Interchain interactions and the staging structure in charge-transfer complexes with neutral-ionic transitions. Synthetic Metals, 2003, 135-136, 629-630.	2.1	0
102	Theoretical study for photoinduced phase transition in superstructures. Synthetic Metals, 2003, 137, 1223-1224.	2.1	0
103	Photoinduced phase transition accelerated by use of two-component nanostructures: A computational study on an Ising-type model. Physical Review B, 2003, 68, .	1.1	7
104	Optical hysteresis in a spin-crossover complex. Physical Review B, 2003, 67, .	1.1	14
105	Dynamical Phase Transition in a Spin–Crossover Complex. Journal of the Physical Society of Japan, 2003, 72, 1615-1618.	0.7	19
106	Conceptual design of nanostructures for efficient photoinduced phase transitions. Applied Physics Letters, 2002, 80, 2562-2564.	1.5	14
107	Theoretical Study of Staging Structure in the Neutral-Ionic Transition of Charge-Transfer Complexes. Phase Transitions, 2002, 75, 831-837.	0.6	2
108	Monte Carlo Simulation for the Photoinduced Phase Transition on a Two-Dimensional Stripe-Structure. Phase Transitions, 2002, 75, 753-758.	0.6	2

#	Article	IF	CITATIONS
109	Theoretical Study of the Charge Transfer Absorption in Cobalt-Iron Cyanide. Molecular Crystals and Liquid Crystals, 2002, 376, 423-429.	0.4	2
110	Mechanism of reversible photo-induced magnetization in prussian blue analogues. Phase Transitions, 2001, 74, 209-233.	0.6	7
111	Magnetic properties of TDAE-C[sub 60] under pressure. AIP Conference Proceedings, 2001, , .	0.3	0
112	Local mechanism of the reversible photo-induced phase transition in Co–Fe prussian blue analogues. AIP Conference Proceedings, 2001, , .	0.3	0
113	Theoretical Study of Pressure Effect on TDAE-C60. Journal of the Physical Society of Japan, 2001, 70, 1892-1895.	0.7	15
114	Novel Mechanism of Photoinduced Reversible Phase Transitions in Molecule-Based Magnets. Physical Review Letters, 2001, 86, 348-351.	2.9	79
115	Crucial effects of intramolecular charge distribution on the neutral-ionic transition of tetrathiafulvalene–p-chloranil. Physical Review B, 2001, 64, .	1.1	15
116	Pressure effect in TDAE-C60ferromagnet: Mechanism and polymerization. Physical Review B, 2001, 63, .	1.1	32
117	The mechanism of the photo-induced magnetic transition in Co–Fe cyanide with ab initio calculations. Journal of Luminescence, 2000, 87-89, 658-660.	1.5	10
118	Ab initiocalculations on the mechanism of charge transfer in Co-Fe Prussian-blue compounds. Physical Review B, 1999, 60, 12990-12993.	1.1	52
119	Theoretical Study for Pressure Effects in Orbital Ordering Ferromagnets. Molecular Crystals and Liquid Crystals, 1997, 306, 169-176.	0.3	О
120	Role of Jahn-Teller Distortion in Magnetic and Optical Properties of TDAE-C60. Synthetic Metals, 1997, 86, 2387-2388.	2.1	5
121	A theoretical model for ferromagnetism of TDAE-C60. Solid State Communications, 1997, 101, 231-235.	0.9	47
122	Pressure Effects in Ferromagnetism of Orbital Ordering Ferromagnet. Journal of the Physical Society of Japan, 1997, 66, 2487-2495.	0.7	9
123	Spin-Polarized Band Sturcture for Organic Molecular Crystals. Molecular Crystals and Liquid Crystals, 1996, 286, 211-216.	0.3	0
124	Theoretical study on possibility of organic metallic ferromagnetism. Synthetic Metals, 1995, 71, 1789-1790.	2.1	12
125	First-Principles Band Structure Calculation for Organic Molecular Crystals. Molecular Crystals and Liquid Crystals, 1995, 272, 161-165.	0.3	2
126	Dipole-Dipole Interaction and Field-Induced Phase Transition in Molecular Antiferromagnet MOTMP. Journal of the Physical Society of Japan, 1994, 63, 3158-3162.	0.7	9

#	ARTICLE	IF	CITATIONS
127	THE ELECTRONIC BAND STRUCTURES FOR AN ANTIFERROMAGNETIC STATE OF Cu2Sb-TYPE INTERMETALLIC COMPOUND Cr2As. International Journal of Modern Physics B, 1993, 07, 770-773.	1.0	1
128	Color-Switchable Glass and Display Devices Fabricated by Liquid Processes with Electrochromic Nanoparticle "Ink― Applied Physics Express, 0, 1, 104002.	1.1	44